Magnetic study of nano-crystalline cobalt substituted Mg-Mn ferrites processed via solution combustion technique

Gagan Kumar[1*], Ritu Rani[1], Vijayender Singh[1], Sucheta Sharma[1], Khalid M. Batoo[2], M. Singh[1]

[1]*Department of Physics, Himachal Pradesh University, Shimla, 171005, India*
[2]*King Abdullah Institute for Nanotechnology, King Saud University, P. O. Box 2460, Riyadh, 11451, Saudi Arabia*

*Corresponding author. Tel: (+91) 9816418069; Fax: (+91) 01792 266097; E-mail: bhargava_phy_hpu@yahoo.co.in

ABSTRACT

Co^{2+} substituted Mg-Mn nanoferrites having formulae $Mg_{0.9}Mn_{0.1}Co_xFe_{2-x}O_4$, where x = 0.0, 0.1, 0.2 & 0.3, have been prepared for the first time by solution combustion technique. The magnetic properties of nanoferrites such as M-H, initial permeability (μ_i) and magnetic loss tangent (*tan δ*) have been investigated as a function of frequency in the range 700 Hz to 30 MHz. X-ray diffraction patterns confirmed the formation of single phase spinel structure of all the nanoferrites. The surface morphology of the samples is studied by using scanning electron microscopy (SEM), while elemental compositions of samples are studied by energy dispersive X-ray analysis (EDAX). Saturation magnetization (M_s) and magneto-crystalline anisotropy constant (K_1) are found to be increasing with an increase in cobalt content while initial permeability and magnetic loss tangent are found to be decreasing with an increase in frequency as well as with the increasing concentration of Co^{2+} ions. The very low values of magnetic loss tangent even at high frequencies are the prime achievements of the present work. Copyright © 2013 VBRI press.

Keywords: Mg-Mn nanoferrites; X-ray diffraction; M-H; initial permeability.

Gagan Kumar has obtained his M. Sc. from Himachal Pradesh University Shimla and pursuing his Ph. D. in physics from the same university under the supervision of Professor Mahavir Singh. His area of research includes structural, electric, dielectric and magnetic properties of bulk and nanoferrites. At present he is working as Head Department of Applied Sciences at Green Hills Polytechnic College Solan (H.P).

K. M. Batoo received his Ph.D. in Applied Physics from Aligarh Muslim University, Aligarh, India. His research interests are focused on Magnetic nanomaterials, Spintronic, Multiferrioc and Magnetoelectric Materials, Magnetic multilayer's (MTJs as GMR) and Magnetic layered double hydroxide (MLDH).

M. Singh did his Ph.D. in physics from Himachal Pradesh University Shimla in collaboration with Indian Institute of Technology, New Delhi, India in 1995 and M.Phil. in 1990 from Himachal Pradesh University Shimla. He is working as Professor in the Department of Physics, Himachal Pradesh University Shimla. He is common wealth fellow and his research is focused on semiconductor oxides, diluted magnetic semiconductors, ferrites and multiferroics.

Introduction

Ferrites with a spinel structure are technologically important class of magnetic oxides due to their good magnetic properties [1]. Applications of nanoferrites are growing in leaps and bounds with advancement in nanotechnology [2]. In recent years, nanoparticles have attracted considerable attentions because of their potential applications in magnetic fluids, high frequency magnets, microwave absorbers, high density data storage, sensors, coolants, optical devices, magnetically guided drug delivery systems, cancer therapy and Magnetic Resonance Image [3]. In ferrites the cations occupy the tetrahedral (A) and octahedral (B) sites and the compositional variation results in the redistribution of metal ions over the tetrahedral and octahedral sites, which can modify the magnetic properties of ferrites. Amongst various ferrites Mg-Mn ferrites are quite versatile from the point of view of their technological applications and have extensive use in the construction of non-reciprocal devices at microwave frequencies such as circulators, gyrators and phase shifetr [4]. As the propeties of ferrites are known to be sensitive to their composition and the processing technique used to synthesize them [5-6] thus, several investigators have synthesized and characterized substituted Mg-Mn ferrites by standard ceramic technique [7], standard solid state reaction technique [8], citrate precursor technique [9] and ball

milling method **[10]**. Inspite of various processing techniques there is no report available on the study of cobalt substituted Mg-Mn nanoferrites by solution combustion technique thus; in the present work we have chosen solution combustion method to synthesize the $Mg_{0.9}Mn_{0.1}Co_xFe_{2-x}O_4$ nanoferrites. The solution combustion technique is a novel synthesis method which enables rapid synthesis of highly substituted oxides. In this method the metal precursors (typically in the form of nitrates serving as oxidizers) is mixed in water with fuel (e.g. glycine) and then heated resulting thereby in self-ignition to yield complex oxides in a one-step process. The advantages of this technique include reactant mixing at the molecular level and the unique ability to tailor product's structural characteristics by varying parameters such as fuel and oxidizer ratio; composition. Although the magnetic properties of mixed Mg–Mn bulk ferrites have been studied extensively **[7-10]**, the available literature on the substituted Mg-Mn nanoferrites is scarce. Further, the magnetic study of cobalt substituted Mg-Mn nanoferrites is not well documented and reported, therefore, in the present investigation, a maiden attempt has been made to investigate the effects of Co^{2+} ions on the magnetic properties of Mg-Mn nanoferrites synthesized by solution combustion method.

Experimental

Materials synthesis and characteristics

$Mg_{0.9}Mn_{0.1}Co_xFe_{2-x}O_4$ where x = 0.0, 0.1, 0.2 & 0.3 are synthesized via solution combustion technique. The chemical reagents used in this work are ferric nitrate, $Fe(NO_3)_3.9H_2O$ (>99%, ACROS Organics, USA), cobalt nitrate $Co(NO_3)_2.6H_2O$ (>99%, RANKEM, India), magnesium nitrate $Mg(NO_3)_2.6H_2O$ (>99%, RANKEM, India), manganese nitrate, $Mn(NO_3)_2.4H_2O$ (>99%, ACROS Organics, USA) and glycine NH_2CH_2COOH (>98.5%, Fisher Scientific, India) as a fuel. In a stoichiometric ratio ferric nitrate, cobalt nitrate, magnesium nitrate, manganese nitrate and glycine are mixed in distilled water to obtain precursor solutions. The obtained precursor solution is then heated on a hot plate, at 40^0C with constant stirring, till the solution starts to burn with release of lots of heat. The obtained powder samples are calcined at 500^0C for 4 h. The calcined powders obtained for all the nanoferrites are then pressed into pallets. The prepared samples are sintered at 700^0C for 4h. Now the torroidal rings of these ferrites having thickness 2 mm and the ratio of outer diameter to inner diameter equal to 1.5 are formed under a pressure of ~5 tons. For measurements of initial permeability and magnetic loss tangent, the torroids are wound with about 52 turns of 32 SWG enameled copper wire. The initial permeability is calculated by using the relation **[11]**

$$\mu_i = L/L_o \qquad (1)$$

where L is measured inductance of the sample and L_o is air core inductance and is expressed as $L_o = 4.6\ N^2d\ log\ (OD/ID) \times 10^{-9}$ henry, N being the number of turns, d is thickness of toroid in meters, OD and ID are outer and inner diameters of the toroids respectively. The

measurements are carried out by making use of Precision LCR meter 4285A in frequency ranging from 0.1 MHz to 30 MHz. The single-phase nature of the prepared samples is checked by x-ray diffraction (XRD) studies, which are made by $Cu-K_\alpha$ radiation of wavelength 1.54 Å using XPERT-PRO X-ray diffractometer and the microstructures of the fractured surfaces are studied using QUANTA 250 FFID 9393. The M-H measurements at room temperature have been performed using Vibrating Sample Magnetometer of Microsense by applying the field from -22000 to 22000 Oe.
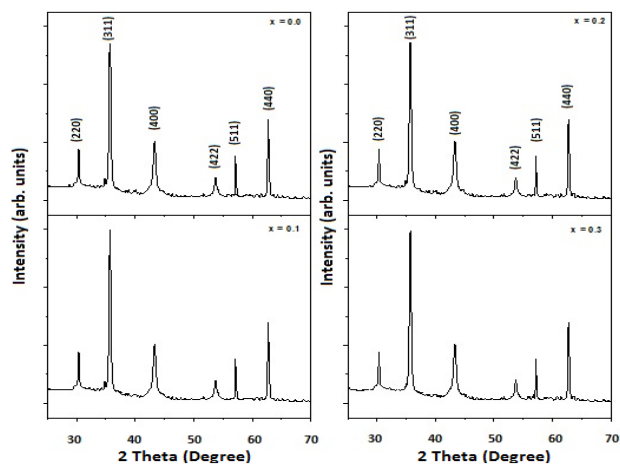

Fig. 1. X-ray diffraction patterns of $Mg_{0.9}Mn_{0.1}Co_xFe_{2-x}O_4$ nanoferrites.
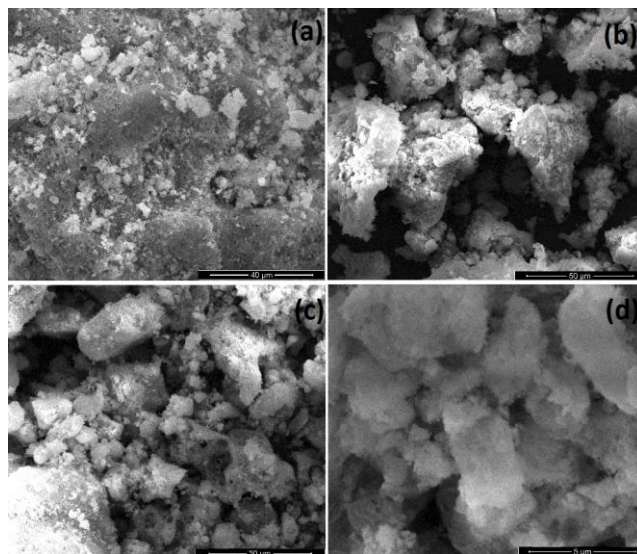

Fig. 2. SEM images of $Mg_{0.9}Mn_{0.1}Co_xFe_{2-x}O_4$ nanoferrites (a) x=0.0, (b) x=0.1, (c) x=0.2 and (d) x=0.3.

Results and discussion

Structural and compositional study

X-ray diffraction patterns indicating (*hkl*) values of each peak for the $Mg_{0.9}Mn_{0.1}Co_xFe_{2-x}O_4$, x = 0.0, 0.1, 0.2 & 0.3, nanoferrites are shown in **Fig. 1** and are corresponding to those of standard pattern of Mg-Mn ferrite with no extra lines, indicating thereby that the samples have a single phase cubic spinel structure and no unreacted constituents are present in the samples. The particle size of the

nanocrystalline samples is found to be increasing with the increasing content of cobalt ions. Further, to see the morphology of the nanoferrites samples, scanning electron micrographs are taken and the **Fig. 2** is showing the same. The detailed structural analysis has been presented by the authors elsewhere [12].
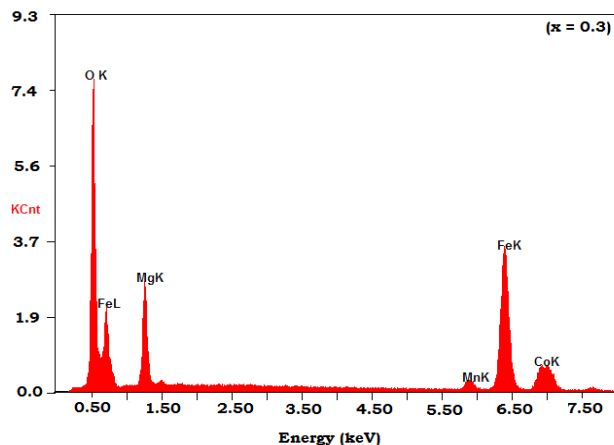

Fig. 3. EDAX pattern of $Mg_{0.9}Mn_{0.1}Co_{0.3}Fe_{1.7}O_4$ nanoferrite.

Table 1. Elemental percentage in $Mg_{0.9}Mn_{0.1}Co_xFe_{2-x}O_4$ nanoferrites.

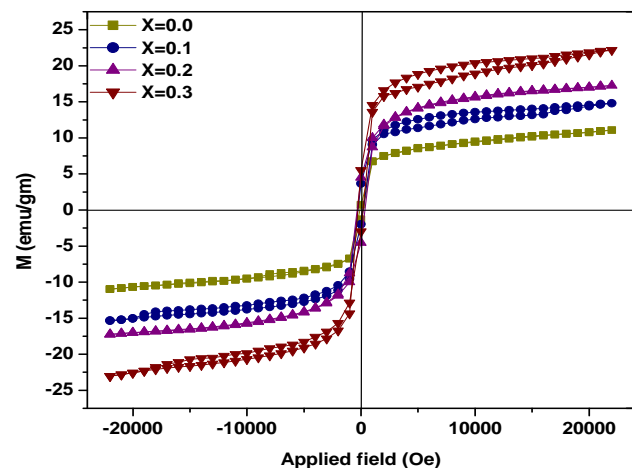| Composition (x)	Mg^{2+} (%)	Mn^{2+} (%)	Co^{2+} (%)	Fe^{3+} (%)	O^{2-} (%)
0.0	10.54	1.24	0.00	35.54	52.68
0.1	11.32	1.44	1.81	32.28	53.15
0.2	15.21	1.50	3.47	26.30	53.52
0.3	17.98	1.53	4.33	22.50	53.66

Fig. 4. M-H curve for $Mg_{0.9}Mn_{0.1}Co_xFe_{2-x}O_4$ nanoferrites.

In order to confirm the chemical composition and stoichiometric proportions of the typical samples of $Mg_{0.9}Mn_{0.1}Co_xFe_{2-x}O_4$ ferrite nanoparticles, energy dispersive analysis of X-ray (EDAX) study is carried out and the typical EDAX spectra for x=0.3 is presented in **Fig. 3**. The compositional percentage of Mg^{2+}, Mn^{2+}, Fe^{3+}, Co^{2+}, and O^{2-} ions presented in the samples are given in **Table 1**. It is observed from **Table 1** that there is no impurity phase exists. All the ions present in $Mg_{0.9}Mn_{0.1}Co_xFe_{2-x}O_4$ (x=0.0,

0.1, 0.2 and 0.3) are in good stoichiometric proportions as desired.

M-H study

Fig. 4 shows the M-H curves for $Mg_{0.9}Mn_{0.1}Co_xFe_{2-x}O_4$, x = 0.0, 0.1, 0.2 & 0.3, nanoferrites at room temperature. The values of saturation magnetization (M_s), remanence magnetization (M_r), coercivity (H_c), remanence ratio (M_r/M_s), magneton number (n_B) and magneto-crystalline anisotropy (K_1) are calculated from these hysteresis plots and their values are given in **Table 2**.

Variations of magneton number

The magneton number (n_B) is calculated from the saturation magnetization of hysteresis loops using relation [9] and is shown in **Table 2**:

$$n_B = \frac{(M \times M_s)}{5585} \quad (2)$$

where M is the molecular weight of particular composition, M_s is saturation magnetization (emu/gm) and 5585 is magnetic factor. It is evident from **Table 2** that n_B is increasing with the increasing substitution of Co^{2+} ions. The increase in n_B with increasing substitution of Co^{2+} ions is because of the high exchange interaction energy and relatively higher orbital contribution of Co^{2+} ions for the magnetic moment.

Variations of magneto-crystalline anisotropy constant

The variations in magneto-crystalline anisotropy constant (K_1) with the increasing substitution of cobalt ions are shown in Table 2 and are calculated from the following relation [13].

$$K_1 = c\, M_s.\, H_a \quad (3)$$

where H_a is anisotropic field and c is taken as -3/4 since K_1 for Mg-Mn ferrite is known to be negative [13]. It is seen from the **Table 2** that K_1 is increasing with an increasing substitution of cobalt ions. These results can be explained on the basis of Single-Ion anisotropy model [9], which shows that Fe^{3+} ions present at A as well as at B sites contribute to the anisotropy energy. The net value of K_1 is given by relative contribution of positive anisotropy of Fe^{3+} ions at tetrahedral site, which is compensated by the negative anisotropy of Fe^{3+} ions at octahedral site. As the concentration of Co^{2+} ions is increased, the cation distribution of Fe^{3+} ions get modified which yields a different number of Fe^{3+} ions present at both the sites which in turn affect K_1. With most ions like Mn^{2+}, Fe^{2+} etc. the orbital moment is quenched and the spin-orbit interaction introduces only a relatively small anisotropy. In Co^{2+}, however, the crystal field is not able to remove the orbital degeneracy and the orbital moment is of the same order of magnitude as the spin moment. This is regarded as the cause of the large anisotropy of cobalt [14].

Variations of saturation magnetization

The variation of saturation magnetization with the increasing concentration of Co^{2+} ions is shown in **Table 2**. According to Neel's model [15] there are three kinds of exchange interactions between unpaired electrons of two ions i.e. A-A interaction, B-B interaction and A-B interaction. A-B interaction heavily predominates over A-A and B-B interactions. A-B interaction aligns all magnetic spins at A-site in one direction and those at B-site in opposite direction. Net magnetic moment of lattice is therefore difference between magnetic moments of B and A sublattices:

$$M = M_B - M_A \qquad (4)$$

Table 2. Saturation magnetization (M_s), Remanence magnetization (M_r), Coercivity (H_c), Remanence ratio (M_r/M_s), Magneton number (n_B) and magneto-crystalline anisotropy (K_1) for $Mg_{0.9}Mn_{0.1}Co_xFe_{2-x}O_4$ nanoferrites.

Composition (x)	0.0	0.1	0.2	0.3
M_s (emu/gm)	10.98	14.49	17.25	21.74
M_r (emu/gm)	1.01	1.48	2.25	2.82
H_c (Oe)	126.7	227.6	228.4	341.6
M_r/M_s	0.09	0.10	0.13	0.13
n_B (μ_B)	0.399	0.528	0.629	0.794
$K_1/10^4$ (erg/gm)	-10.71	-8.69	-7.77	-6.52

As Co^{2+} ions occupy B-sites [4] and replace Fe^{3+} ions due to which magnetization of B-sub lattice decreases keeping magnetization of A-sublattice constant. Thus, resultant magnetization according to equation 4 is supposed to decrease. But, it is evident from **Table 2** that saturation magnetization increases with the increasing concentration of cobalt ions. This increase in saturation magnetization with the increase in cobalt content thus can be explained because of the fact that as Co^{2+} ions are known to give large induced anisotropy, shown in **Table 2**, due to relatively high orbital contribution to the magnetic moment [16] therefore, equation 3 is then justifying the increase in saturation magnetization.

Variations of coercivity

The compositional variations of coercivity are given in **Table 2**, which shows that H_c is increasing with the increasing substitution of cobalt content. This can be explained because of the following equation [17]

$$H_c = a(K_1/M_s) + b(N_1-N_2)M_s + c(\lambda_s\tau/M_s) \qquad (5)$$

Where a, b, c are constants, N_1 and N_2 are demagnetization factors, λ_s is magnetostriction strain and τ is mechanical strain. The first term is because of the magneto-crystalline anisotropy of the material, second term is given by the shape anisotropy of crystalline particles and the third one is originated from the elastic mechanical deformation. The first term plays a major roll for H_c and the contribution of other terms is very small. Since H_c is directly proportional to the magneto-crystalline anisotropy and it is evident that cobalt content is increasing the magneto-crystalline anisotropy, which in turn decreases the domain wall energy resulting thereby high coercivity [16].
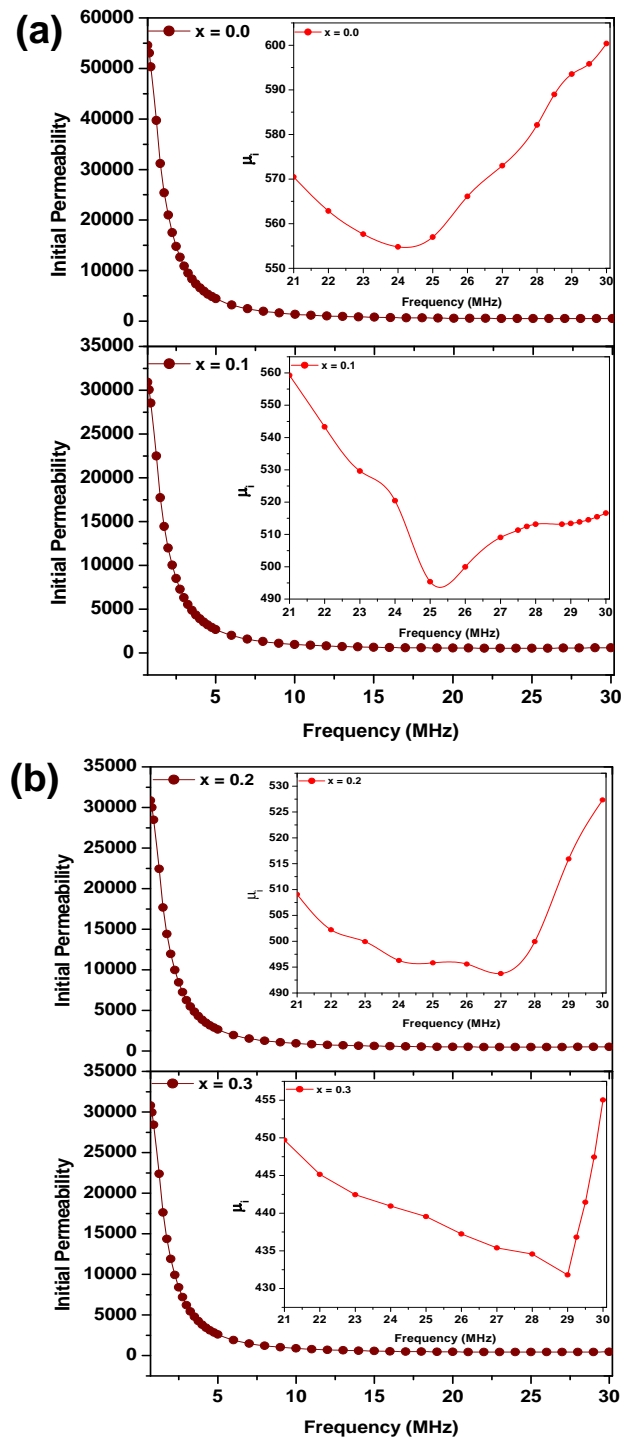

Fig. 5. Variation of initial permeability with frequency for (a) $Mg_{0.9}Mn_{0.1}Co_xFe_{2-x}O_4$ and (b) $Mg_{0.9}Mn_{0.1}Co_xFe_{2-x}O_4$ nanoferrites.

Variations of initial permeability

The typical variations of initial permeability with frequency for all the nanoferrites are shown in **Fig. 5 (a)** and **(b)**. The result, in the inset, shows a rapid increase in μ_i after certain frequency which is indicative of the onset of resonance. When the frequency of the applied magnetic field equals the Larmor precession of the electron spins, resonance occurs and the energy is transferred from the field to the system in orienting the magnetic dipoles. The frequency of the onset of resonance varies with cobalt content; it

increases with the increase in the Co^{2+} ions. This observation is in agreement with Globus model [18]. According to this model, relaxation character is represented as-

$$(\mu_i-1)^2.f_r = \text{constant} \qquad (6)$$

where μ_i is the static initial permeability and f_r is the relaxation frequency. These workers also showed that the transformation of magnetic spectra from the relaxation character to the resonance character changes Eq. (6) to

$$(\mu_i-1)^{1/2}.f_r = \text{constant} \qquad (7)$$

This indicates that higher the permeability values, the lower will be the resonance frequency.
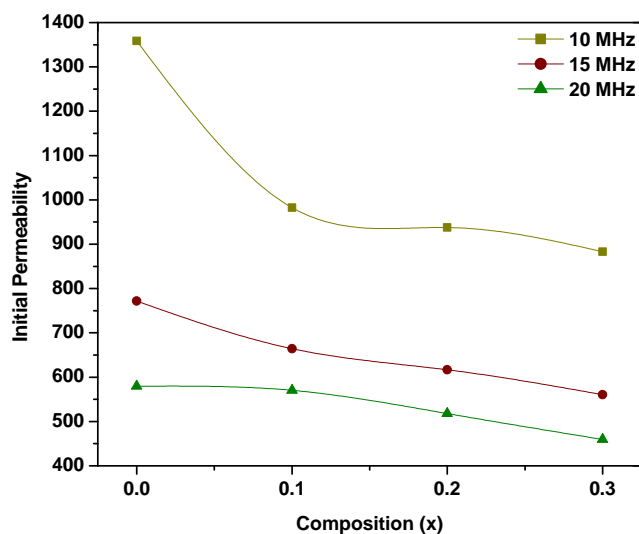
Fig. 6. Variation of initial permeability with composition for $Mg_{0.9}Mn_{0.1}Co_xFe_{2-x}O_4$ nanoferrites at different frequencies.

It was not, however, possible to observe the complete resonance peaks as they seem to appear at frequencies beyond 30 MHz the upper limit of the frequency used in our studies. **Fig. 6** shows the variations of initial permeability with the increasing content of cobalt ions. It is evident from the results that initial permeability is decreasing with the increasing substitution of Co^{2+} ions. This can be explained by the following dependence of initial permeability [19].

$$\mu_i = M_s^2 D_m/K_1 \qquad (8)$$

Where D_m is the average grain diameter, K_1 is the magneto-crystalline anisotropy constant and M_s is the saturation magnetization. As the magneto-crystalline anisotropy is increasing with the increase in cobalt content hence μ_i is expected to decreases with increasing substitution of Co^{2+} ions.

Magnetic loss tangent

Fig. 7 shows the variation of magnetic loss tangent with frequency for $Mg_{0.9}Mn_{0.1}Co_xFe_{2-x}O_4$ nanoferrites. The loss is due to lag of domain walls motion with respect to the

applied alternating magnetic field and is attributed to imperfections in the lattice. The results revel that magnetic loss tangent (tan δ) decreases initially with frequency reaching a minimum value, and then start to increase thereafter. The frequency at which tan δ is minimum is called the threshold frequency. The increase in tan δ shows the tendency for a resonance loss peak, which will occur at frequencies higher than those used in present study. **Fig. 8** shows the variation of magnetic loss tangent with composition for $Mg_{0.9}Mn_{0.1}Co_xFe_{2-x}O_4$ nanoferrites at different frequencies. It is evident from the variations that tan δ is decreasing with an increasing substitution of Co^{2+} ions. The major contribution to the magnetic losses in ferrites is due to hysteresis losses [20], which in turn are based on damping phenomenon associated with irreversible wall displacement and spin rotations. However, the hysteresis loss becomes less important in the high-frequency range because the wall displacement is mainly damped and the hysteresis loss will be due to spin rotation.
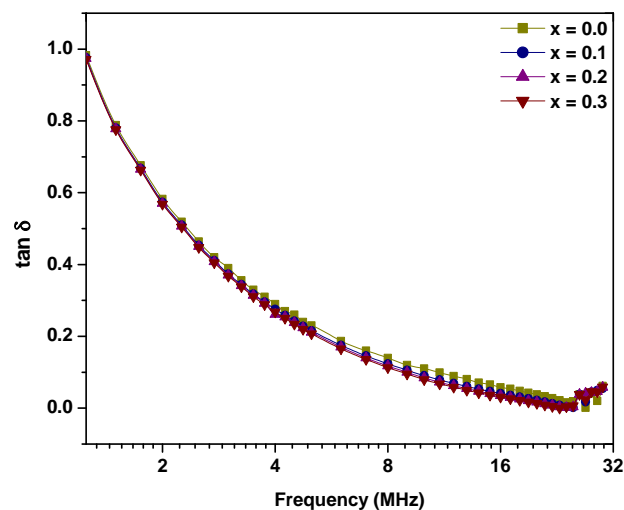

Fig. 7. Variation of magnetic loss tangent with frequency for $Mg_{0.9}Mn_{0.1}Co_xFe_{2-x}O_4$ nanoferrites.
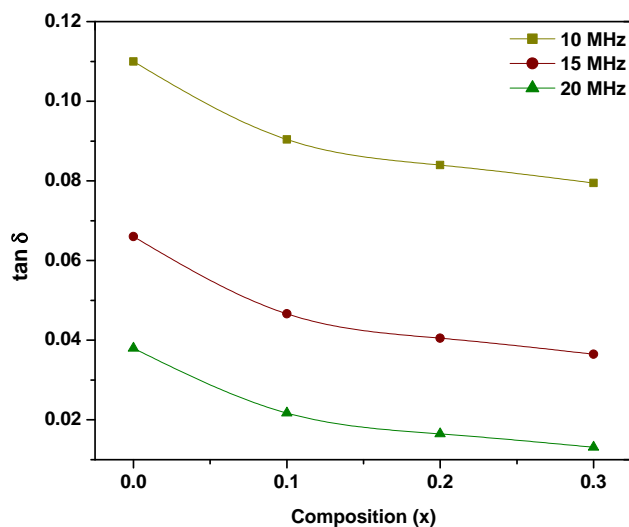

Fig. 8. Variation of magnetic loss tangent with composition for $Mg_{0.9}Mn_{0.1}Co_xFe_{2-x}O_4$ nanoferrites at different frequencies.

The values of magnetic loss tangent are found to be small even at higher frequencies for these samples, which is one of the criteria for the materials to be used in microwave devices and for deflection yoke. Further, the results of the present study reveals that magnetic properties improved as compared to those reported earlier **[21]** for the same composition, $Mg_{0.9}Mn_{0.1}Fe_2O_4$, prepared by conventional ceramic method. **Table 3** gives the comparison of initial permeability and relative loss factor for the sample prepared by conventional and solution combustion technique. It is revealed from the table that initial permeability has increased by 39-46 times and relative loss factor is reduced by two orders of magnitude for the sample synthesized by the solution combustion technique.

Table 3 Comparison of initial permeability and relative loss factor for the sample prepared by conventional and solution combustion technique.

	Conventional ceramic method	Solution combustion technique
	At 10 MHz	At 10 MHz
Initial permeability	~30-35	1358.26
Relative loss factor	$\sim 6.5 \times 10^{-3}$	8.1×10^{-5}

Conclusion

Cobalt substituted Mg-Mn nanoferrites were successfully synthesized by solution combustion technique. Saturation magnetization, magneton number and magneo-crystalline anisotropy were found to be increasing with the increasing substitution of Co^{2+} ions while initial permeability and magnetic loss tangent were observed to be decreasing with the increase in cobalt content. $Mg_{0.9}Mn_{0.1}Fe_2O_4$ ferrite sample was observed to show remarkably higher values of initial permeability and very low relative loss factor than the sample prepared by the conventional ceramic technique.

Reference

1. Shirsath, S. E.; Jadhav, S. S.; Toksha, B. G.; Patange, S. M.; Jadhav, K. M.; *Scr. Mater.* **2011**, 64**,** 773.
   DOI: 10.1016/j.scriptamat.2010.12.043
2. Tiwari, Ashutosh.; *Adv. Mater. Lett.* **2012**, 3(1), 1.
   DOI: 10.5185/amlett.2012.13001
3. Tiwari, Ashutosh.; Mishra, Ajay K.; Kobayashi, Hisatoshi; Turner, Anthony, P.F.; *Intelligent Nanomaterials* Wiley-Scrivener Publishing LLC, USA, 2012, ISBN 978-04-709387-99.
4. Kumar, Gagan; Kanthwal, M.; Chauhan, B. S.; Singh, M.; *Indian J. Pure & Appl. Phys.* **2006**, 44, 930.
5. Kumar, Gagan; Chand, J.; Verma, S.; Singh, M.; *J. Phys. D: Appl. Phys.* **2009**, 42, 155001.
   DOI: 10.1088/0022-3727/42/15/155001
6. Kumar, S.; Shinde, T. J.; Vasambekar, P. N.; *Adv. Mat. Lett.* **2013**, 4(5), 373.
   DOI: 10.5185/amlett.2012.10429
7. Lakshman, A.; Subba Rao, P. S. V.; Rao, K. H.; *J. Magn. Magn. Mater.* **2004**, 284, 352.
   DOI: 10.1016/j.jmmm.2004.06.058
8. Sharma, S. K.; Kumar, R.; Kumar, V. V. S.; Knobel, M.; Reddy, V. R.; Gupta, A.; Singh, M.; *Nucl. Instr. and Meth. B.* **2006**, 248, 37.
   DOI: 10.1016/j.nimb.2006.03.188
9. Chauhan, B. S.; Kumar, R.; Jadhav, K. M.; Singh, M.; *J. Magn. Magn. Mater.* **2005**, 283, 71.
   DOI: 10.1016/j.jmmm.2004.04.133
10. Sharma, S. K.; Kumar, R.; Kumar, S.; Knobel, M.; Meneses, C. T.; Kumar, V. V. S.; Reddy, V. R.; Singh, M.; Lee, C. G.; *J. Phys. Condens. Matter.* **2008**, 20, 235214.
    DOI: 10.1088/0953-8984/20/23/235214
11. Keluskar, S. H.; Tangsali, R. B.; Naik, G. K.; Budkuley, J. S.; *J. Magn. Magn. Mater.* **2006**, 305, 296.
    DOI: 10.1016/j.jmmm.2006.01.018
12. Kumar, Gagan; Rani, Ritu; Sharma, S.; Batoo, K. M.; Singh, M.; *Ceram. Inter.* **2013**, 39, 4813.
    DOI: 10.1016/j.ceramint.2012.11.071
13. Kang, Sun-Ho; Yoo, Han-Ill.; *J. Appl. Phys.* **2000**, 88, 4754.
    DOI: 10.1063/1.1312844
14. Kumar, Gagan; Chand, J.; Dogra, Anjana; Kotnala, R. K.; Singh, M.; *J. Phys. Chem. Solids* **2010**, 71, 375.
    DOI: 10.1016/j.jpcs.2010.01.003
15. Neel, L.; *Ann. Phys.* **1948**, 3, 137.
16. Devan, R. S.; Kolekar, Y. D.; Chougule, B. K.; *J. Phys. Condens. Matter.* **2006**, 18, 9809.
    DOI: 10.1088/0953-8984/18/43/004
17. Dung, N. K.; Tuan, N. H.; *VNU J. Sci. Maths-Phys.* **2009**, 25, 153.
18. Mathur, P.; Thakur, A.; Singh, M.; *J. Phys. Chem. Solids.* **2008**, 69, 187.
    DOI: 10.1016/j.jpcs.2007.08.014
19. Globus, A.; Duplex, P.; Guyot, M.; *IEEE Trans. Magn. Magn.* **1971**, 7, 617.
    DOI: 10.1109/TMAG.1971.1067200
20. Chand, J.; Kumar, Gagan; Kumar, P.; Sharma, S. K.; Knobel, M.; Singh, M.; *J. Alloys & Compds.* **2011**, 509, 9638.
    DOI: 10.1016/j.jallcom.2011.07.055
21. Lakshman, A.; Subba Rao, P. S. V.; Rao, K. H.; *J. Magn. Magn. Mater.* **2004**, 283, 329.
    DOI: 10.1016/j.jmmm.2004.05.040